15. BASE OF LARGE *GEPHYROCAPSA* AND ASTRONOMICAL CALIBRATION OF EARLY PLEISTOCENE SAPROPELS IN SITE 967 AND HOLE 969D: SOLVING THE CHRONOLOGY OF THE VRICA SECTION (CALABRIA, ITALY)[1]

L.J. Lourens,[2] F.J. Hilgen,[3] and I. Raffi[4]

ABSTRACT

Calcareous plankton biochronology and the astronomical calibration of sapropels are presented for the early Pleistocene in Ocean Drilling Program (ODP) Site 967 and Hole 969D with the aim to solve the existing chronology problem in the Pliocene/Pleistocene boundary stratotype section of Vrica, Italy. Detailed sapropel correlations between these ODP sites and the Vrica and Singa sections, corroborated by calcareous plankton biostratigraphy, indicate that the Vrica section is continuous and that the base of the large *Gephyrocapsa* is diachronous on a global scale.

INTRODUCTION

Recently, two alternative age models were presented for the Pleistocene part of the Pliocene/Pleistocene boundary stratotype section at Vrica (Calabria, southern Italy; Lourens et al., 1996a). The chronology of both models is based on the correlation of characteristic sapropel patterns to the average of the June and July (summer) insolation time series at 65°N of the La90$_{(1,1)}$ (Laskar et al., 1993) astronomical solution (Lourens et al., 1996a, 1996b). The first age model is based on the assumption that the succession at Vrica is continuous. According to this model, the position of almost all calcareous plankton datum planes relative to the oxygen isotope stages is in good agreement with that found in the adjacent northern Atlantic. The only exception is the base of large *Gephyrocapsa* (blG), which is found in Stage 55 in the Vrica and Singa sections (Calabria, southern Italy), whereas it occurs in Stage 48 (or the top of 49) in the open ocean (Raffi et al., 1993). This unexpectedly large discrepancy in age of the blG in the eastern Mediterranean and the open ocean cast serious doubt on the validity of this age model. As a consequence, we developed an alternative age model based on the assumption that the blG is globally (near-)synchronous. This model implies a major hiatus between the top of *Calcidiscus macintyrei* (tCm) and the blG in the Vrica and Singa sections. Application of this alternative model, however, leads to significant discrepancies in the position of the other calcareous plankton events.

In this paper, we aim to solve the astronomical calibration of the sapropels and thereby the existing problem of the two conflicting age models for the Pleistocene part of the Vrica section. For this purpose, we established a high-resolution biochronology for Ocean Drilling Program (ODP) Site 967 and Hole 969D for the same time interval based on an unambiguous correlation of sapropel patterns to the La90$_{(1,1)}$ summer insolation curve at 65°N. To explore the possibility of a blG diachroneity, we also checked the position of this event in a high-resolution sample set of ODP Site 926 from the equatorial Atlantic.

SITE 967 AND HOLE 969D

Site 967 is situated south of Cyprus on the northern flank of a small (~300 m high) ridge near the foot of the northern slope of the Eratosthenes Seamount (34°04′N, 32°43′E) at a water depth of 2554 m (Fig. 1). The top 125 m of the section consists of early Pliocene to Holocene pelagic sediments and contains 80 sapropels and several intervals with mud turbidites. The sediments are relatively undisturbed, but show some small high-angle faulting and a slumped interval associated with an overlying debris-flow unit.

Hole 969D was drilled on the Mediterranean Ridge about 100 km south of the island of Crete (33°50′N, 24°53′E) at a water depth of 2192 m (Fig. 1). The sediments of Pliocene to Holocene age consist of nannofossil oozes and nannofossil clays and contain more than 80 sapropels. The sapropels occur in five distinct groups, which are separated by intervals of yellowish brown sediment that is commonly oxidized and does not contain (preserved) sapropels. In contrast to those of Holes 969A, 969B, and 969E, the sapropels recovered from Hole 969D are intact and undeformed.

BIOSTRATIGRAPHY

We carried out our own high-resolution biostratigraphic study for the tCm, blG, and the top of large *Gephyrocapsa* (tlG) and top of
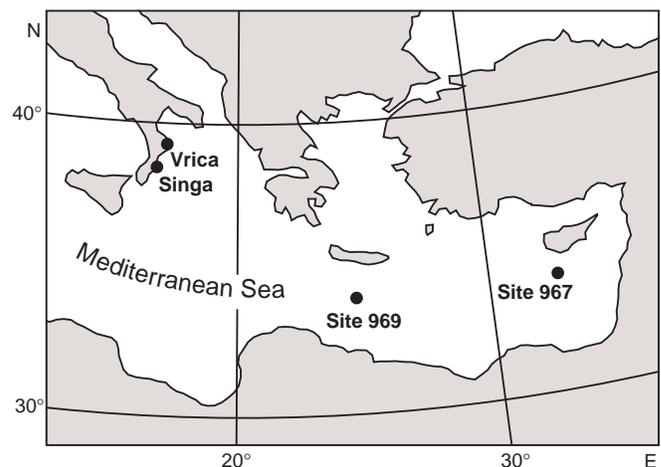

Figure 1. Location map of the studied sections and ODP sites.

Helicosphaera sellii (tHS) in Site 967 and Hole 969D to prevent the use of different taxonomic concepts in this study and that of the Vrica section. In addition, we determined the first occurrence (FO) of the benthic foraminifer species *Hyalinea balthica,* checked for short influxes of the planktonic foraminifer species *Globorotalia crassaformis* and *Globorotalia truncatulinoides,* and counted the number of left-coiling neogloboquadrinids relative to their right-coiling counterpart. Finally, we determined the top of *Discoaster brouweri* (tDb) in Hole 969D and adopted the position of this event in Holes 967A and 967C from the initial shipboard scientific results (Emeis, Robertson, Richter, et al., 1996) and from Staerker (Chap. 31, this volume), respectively. All biostratigraphic data are reported in Figure 2 and Table 1.

The tCm is found between Samples 160-967C-5H-7, 0–2 cm, and 10–12 cm, and Samples 160-969D-4H-6, 49–51 cm, and 58–60 cm. The bIG is placed between Samples 160-967C-5H-6, 30–32 cm, and 40–42 cm, and between Samples 160-969D-4H-5, 100–102 cm, and 110–112 cm. The percentage of large *Gephyrocapsa* increases gradually upwards and show a more complex extinction pattern, i.e., in agreement with the pattern found in other marine sequences of the Mediterranean and open ocean (Raffi et al., 1993; Lourens et al., 1996a). The tIG is placed between Samples 160-967A-5H-1, 95–97 cm, and 115–117 cm, and between Samples 160-969D-3H-6, 45–47 cm, and 75–77 cm. The last occurrence of *H. sellii* is closely associated with the tIG and is placed between Samples 160-967A-5H-1, 105–107 cm, and 115–117 cm, and between Samples 160-969D-3H-
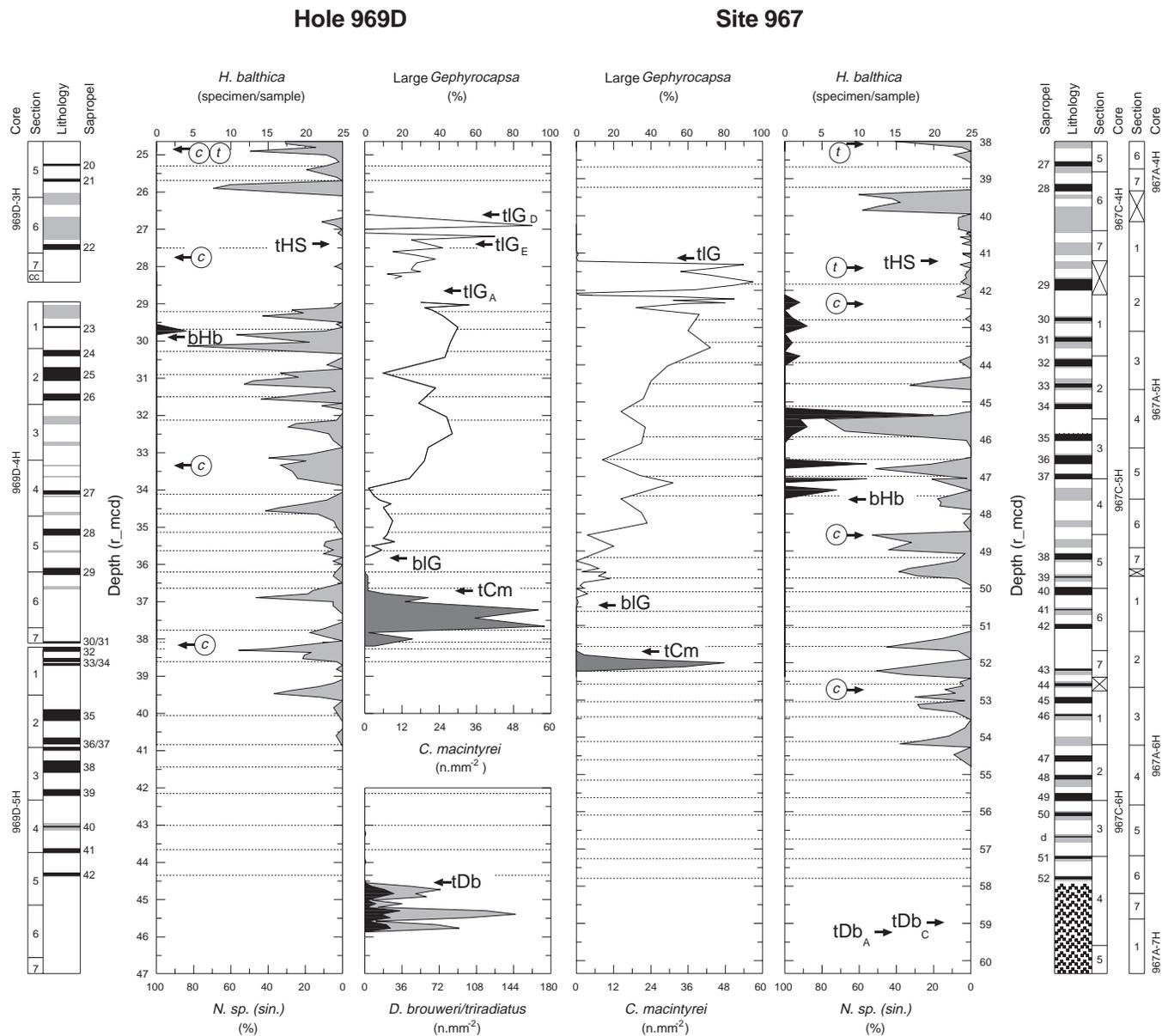

Figure 2. Biostratigraphic data of Site 967 and Hole 969D. Solid intervals in the lithology indicate sapropels, whereas the shaded areas indicate grey layers or less-distinct sapropels. The percentage of large-sized *Gephyrocapsa* (>5.5 μm) is related to 100 *Gephyrocapsa* >4 μm. The percentage of left-coiling neogloboquadrinids (*N.* sp. [sin.]) is related to the total of left and right-coiling neogloboquadrinids. The percentage of *Discoaster triradiatus* (solid) is relative to the total of *Discoaster brouweri* and *D. triradiatus.* Influxes of *Globorotalia crassaformis* and *Globorotalia truncatulinoides* are indicated by *c* and *t,* respectively. The jagged pattern at the bottom of the lithology column of Site 967 indicates a slumped interval.

Table 1. Position and astronomical ages of biostratigraphic datums in Site 967, Hole 969D, and the Vrica section.

Biostratigraphic datum	Event	Vrica Age (Ma)	Site 967 Depth (rmcd)	Site 967 Age (Ma)	Hole 969D Depth (rcmd)	Hole 969D Age (Ma)
Planktonic foraminifers						
Globorotalia truncatulinoides	Influx		38.06	1.145	24.80	1.140
Globorotalia crassaformis	Influx		37.76	1.135	24.80	1.140
Neogloboquadrina sp. (sinistral)	Reappearance	1.220	39.90	1.209	26.01	1.203
Globorotalia truncatulinoides	Influx		41.36	1.262		
Globorotalia crassaformis	Influx		42.35	1.299	27.75	1.295
Neogloboquadrina sp. (sinistral)	Disappearance	1.367	44.38	1.370	29.13	1.371
Globorotalia crassaformis	Influx		48.57	1.539	33.30	1.537
Globorotalia crassaformis	Influx	1.723	52.72	1.722	38.19	1.727
Neogloboquadrina sp. (sinistral)	FCO	1.799	54.23	1.793	39.51	1.789
Calcareous nannoplankton						
Helicosphaera sellii	Top	1.235	41.27	1.259	27.35	1.273
Gephyrocapsa (>5.5 μm)	Top	1.238	41.22	1.257	26.75	1.241
Gephyrocapsa (>5.5 μm)	Base	1.608	50.42	1.616	35.75	1.626
Calcidiscus macintyrei	Top	1.671	51.72	1.673	36.75	1.663
Discoaster brouweri	Top	1.947			44.60	1.953
Benthic foraminifers						
Hyalinea balthica	FCO	1.493	47.50	1.492	29.73	1.403
Polarity reversals						
Upper Olduvai		1.785				
Lower Olduvai		1.942				

Note: FCO = first common occurrence.

6, 114−115 cm, and 125−127 cm. Finally, we placed the tDb and the associated drop in *Discoaster triradiatus* between Samples 160-969D-5H-5, 85−87 cm, and 95−97 cm.

Benthic foraminifers are scarce in Hole 969D and rare specimens of *H. balthica* are present in one sample only. *H. balthica* occurs more frequently in Site 967, although still in very low numbers and discontinuously. *Islandiella ionica,* another benthic foraminifer marker species (Verhallen, 1991), was not found. Several short peak occurrences of *G. crassaformis* and *G. truncatulinoides* were found (Table 1). The first substantial increase of left-coiling neogloboquadrinids is found between Sapropels 34 and 35 in Hole 969D and at a correlative level between Sapropels 46 and 47 in Site 967. An absence interval of this species is present between 26 and 29 revised meters composite depth (rmcd) in Hole 969D and between 40 and 44 rmcd in Site 967 (Fig. 2).

SAPROPEL CHRONOLOGY

A first-order calibration of sapropels to the astronomical record is based on the correlation of large groups or clusters of sapropels in Site 967 and Hole 969D to 400-k.y. maxima in the eccentricity of the Earth's orbit. Four distinct clusters are found between 95 and 40 rmcd in Site 967, and between 90 and 20 rmcd in Hole 969D. Biostratigraphic data indicate that these clusters correspond to the large-scale O, A, B, and C clusters from classical marine sections in southern Italy (e.g., Hilgen, 1991).

The oldest sapropels of the C cluster (i.e., C1−C9 in Singa and *-h in Vrica) can easily be identified in ODP Site 967 (i.e., Sapropels 44−52) and Hole 969D (i.e., Sapropels 30−42; Fig. 3). The next small-scale cluster displays a cyclic alternation of distinct and less-distinct sapropels (i.e., Sapropels 38−42) in Site 967 and of sapropels and grey layers (i.e., Sapropels 27−29) in Hole 969D. These alternating distinct and less-distinct (grey) sapropel patterns can be explained by the interference between precession and obliquity, which is clearly reflected in the La90$_{(1,1)}$ summer insolation curve (Fig. 3): distinct sapropels are correlated to high-amplitude insolation maxima, and less-distinct (grey) sapropels are correlated to low-amplitude insolation maxima (Lourens et al., 1996b). Starting from this second-order calibration, all younger sapropels (i.e., 20−26 in Hole 969D and 27−37 in Site 967) can be correlated directly to the astronomical target curve (Fig. 3). The

Table 2. Position and astronomical ages of sapropels in Site 967 and Hole 969D.

i-cycle	Site 967 Sapropel	Site 967 Depth (rmcd)	Site 967 Age (Ma)	Hole 969D Sapropel	Hole 969D Depth (rmcd)	Hole 969D Age (Ma)
110	27	38.61	1.164	20	25.27	1.164
112	28	39.25	1.185	21	25.68	1.185
122	29	41.85	1.280	22	27.48	1.280
126	30	42.78	1.315			1.315
128	31	43.32	1.335			1.335
130	32	43.95	1.356			1.356
132	33	44.56	1.376			1.376
134	34	45.12	1.398	23	29.63	1.398
138	35	45.95	1.429	24	30.33	1.429
140	36	46.54	1.449	25	30.89	1.449
142	37	47.00	1.471	26	31.51	1.471
152	38	49.15	1.564	27		1.564
154	39	49.70	1.584			1.584
156	40	50.08	1.603	28	34.07	1.603
158	41	50.58	1.622			1.622
160	42	51.03	1.642	29	35.13	1.642
166	43	52.19	1.694			1.694
168	44	52.59	1.715	30/31	38.24	1.715
170	45	53.01	1.736	32	38.25	1.736
172	46	53.41	1.757	33/34	38.62	1.757
176	47	54.57	1.808	35	40.05	1.808
178	48	55.08	1.829	36/37	0.83	1.829
180	49	55.61	1.851	38	41.43	1.851
182	50	56.07	1.872	39	42.12	1.872
184	d	56.68	1.900	40	43.04	1.900
186	51	57.23	1.923	41	43.69	1.923
188	52	57.78	1.944	42	44.32	1.944

Notes: i-cycle codification after Lourens et al., 1996b. Ages refer to the midpoints of the sapropel (Sakamoto et al., Chap. 24, this volume) and represent 3-k.y. lagged ages of the correlative summer insolation maxima.

proposed astronomical calibration provides very accurate numerical ages not only for the sapropels (Table 2; Fig. 3B), but also for the recorded biostratigraphic datum planes (Table 1).

DISCUSSION AND CONCLUSIONS

In the Vrica section, complicating factors like the influence of obliquity, changes in sedimentation rate, and the increasing number of sapropels per large-scale cluster hinder a straightforward astro-
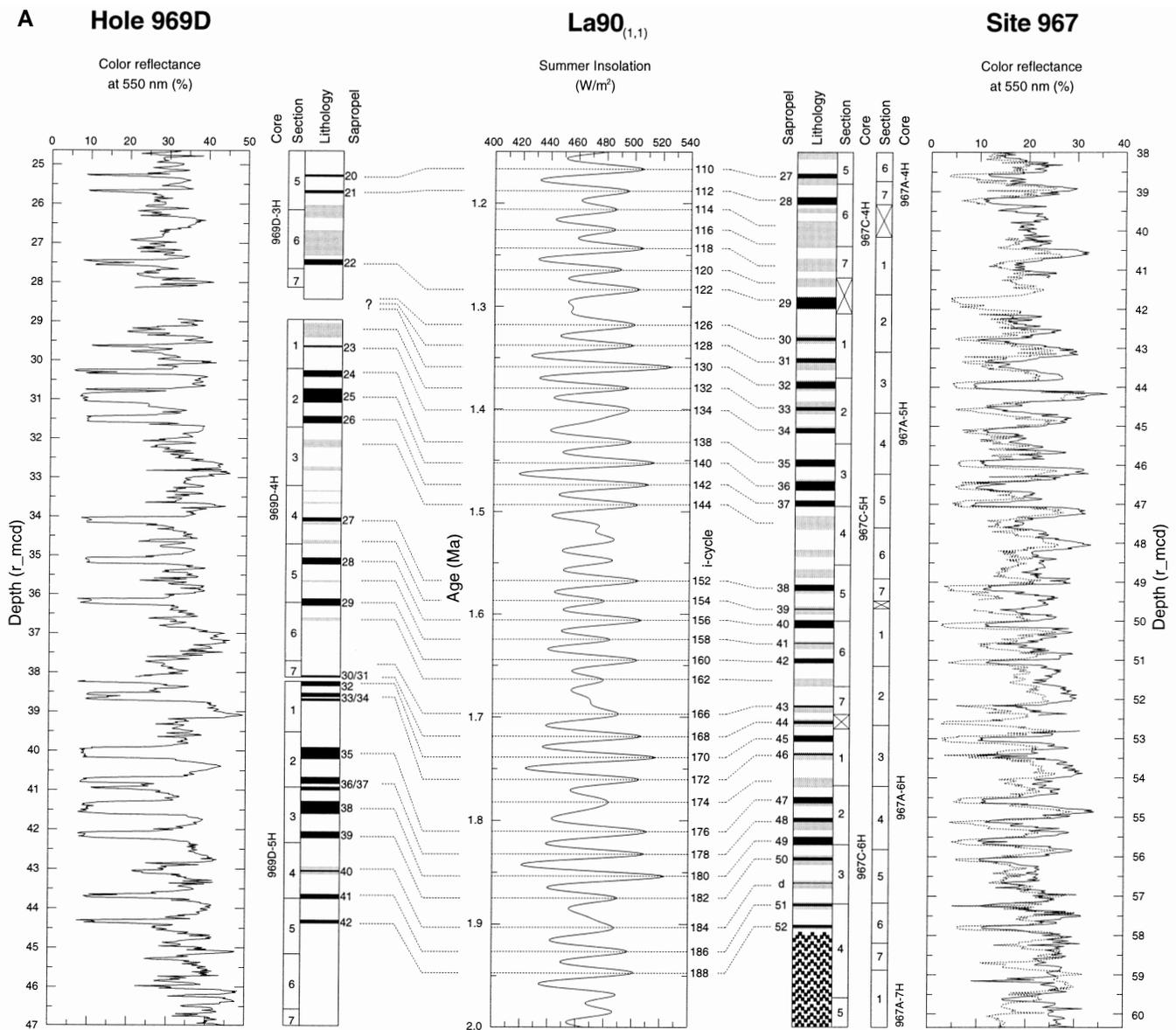
Figure 3. Calibration of early Pleistocene sapropels in Site 967 and Hole 969D to the La90$_{(1,1)}$ (Laskar et al., 1993) summer insolation curve at 65°N against (**A**) depth and (**B**) age. The color reflectance data of Hole 967A (dashed line in right column) has been shifted to the left with 10% relative to that of Hole 967C (solid line) for clarity. All color reflectance data are obtained from Sakamoto et al. (Chap. 24, this volume). The coding (i-cycle) indicated at the right side of the insolation curve is from Lourens et al. (1996b). The jagged pattern in the lithology column of Site 967 indicates a slumped interval.

nomical calibration of the youngest (n–v) sapropels (Hilgen, 1991; Lourens et al., 1996a). A key problem in establishing a sapropel chronology for this part of the Vrica section is the interpretation of the small-scale sapropel cluster n-o-p. According to the continuous age model, as referred to in the introduction, this cluster is not related to a 100-k.y. eccentricity maximum, as could be expected from late Pleistocene phase relations, but reflects an interference pattern between precession and obliquity at the time of the 400-k.y. eccentricity minimum around 1.4 Ma. Starting from this age model, all sapropel correlations between the Vrica and Singa sections and ODP Site 967 and Hole 969D are straightforward and confirmed by biostratigraphic correlations (Fig. 4). The cyclostratigraphic correlation of Sapropels n-o-p with the characteristic interference pattern observed in Site 967 and Hole 969D is biostratigraphically confirmed by the position of tCm and blG and by influxes of *G. crassaformis* (Fig. 4A). The short influx above this group of sapropels is substantiated by rare *G. cras-*

saformis in two successive samples above Sapropel C12 in the Singa section, but was not found in the Vrica section, possibly due to lack of sample resolution. Also, the correlation of the younger sapropels is easily accomplished. It shows that, as in the preceding interval, additional cycles are developed at the ODP sites either as grey layers or as thin indistinct sapropels. All correlations are confirmed by the position of the tDb, tlG, tHS (Fig. 4A) and by the characteristic abundance pattern of left-coiling neogloboquadrinids (Fig. 4B). Similar to the pattern observed in the Vrica section and North Atlantic Deep Sea Drilling Project (DSDP) Site 607, the peak occurrences of left-coiling neogloboquadrinids in Site 967 and Hole 969D are associated with glacial Stages 64 to 44, followed by an interval in which such (peak) occurrences are markedly absent. The next two younger peak occurrences, associated with glacial Stages 36 and 34 in the Atlantic (see Lourens et al., 1996a), are observed in the top part of the studied cores (Fig. 4B). The only remarkable difference between Vrica and
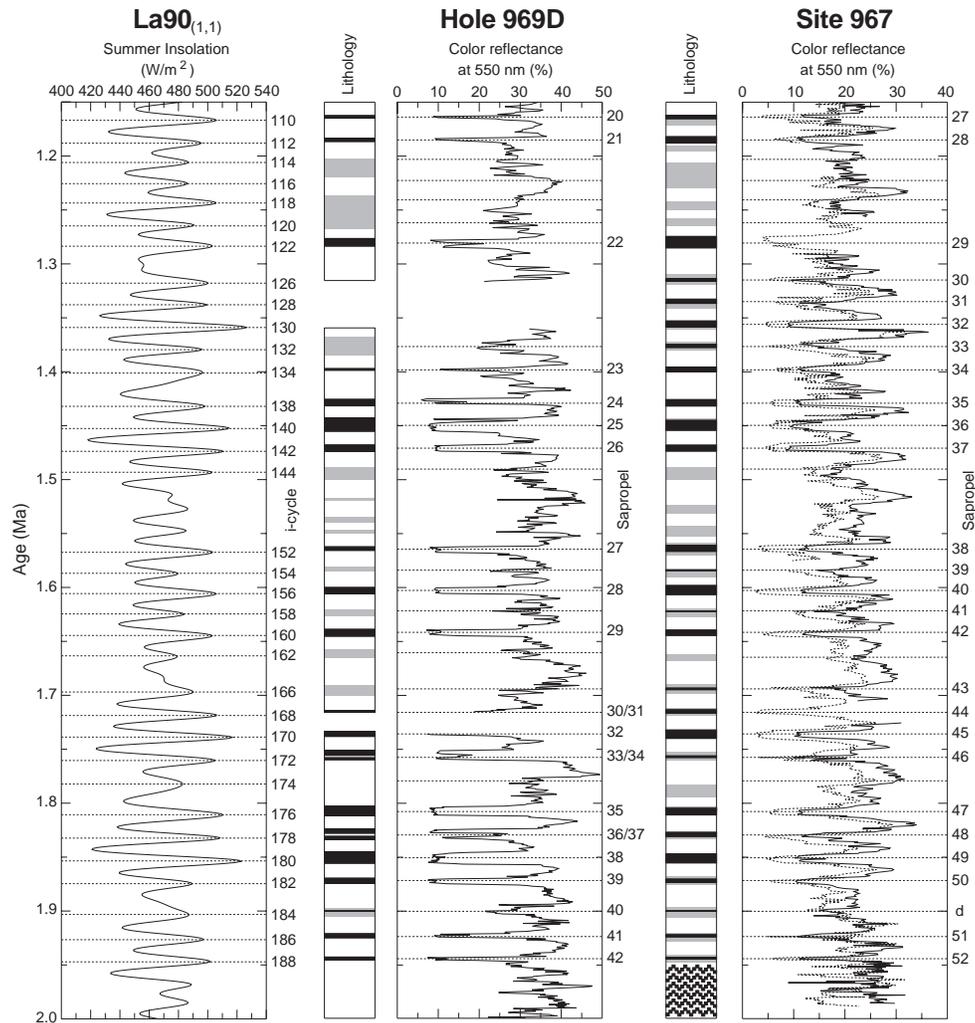
Figure 3 (continued).

the ODP sites is that the pattern of Sapropels q-r-s in the Vrica section (with r being thinner and less prominent)—thought to be indicative of interference between precession and obliquity—is not confirmed at Site 967 and Hole 969D where the three correlative sapropels are equally distinct. At present, we do not have an explanation for this difference.

On the contrary, serious inconsistencies are found if we start from the alternative age model for the Vrica section. This age model, which started from the assumption that blG is globally (near-)synchronous, implied that a major hiatus is present in the interval between tCm and blG (Lourens et al., 1996a). A hiatus, however, is no longer tenable, because the sapropel patterns and bioevents (e.g., the first appearance of large *Gephyrocapsa*, the absence interval of glacial-bound influxes of left-coiling neogloboquadrinids and the tlG and tHS) are remarkably consistent throughout the eastern Mediterranean (Fig. 4).

To investigate the potential global diachroneity of blG, we checked the position of this event in a high-resolution sample set of ODP Site 926 (Ceara Rise, equatorial Atlantic). A comparison of our first results with the age model obtained from orbitally tuned susceptibility records (Bickert et al., 1997) reveals that the blG at this site is considerably older than the global estimate of 1.48 Ma for this event as well (Raffi et al., 1993). The age of 1.59 Ma at Site 926 is only 30 k.y. younger than our estimate for the blG at Sites 967 and 969 in the eastern Mediterranean. In conclusion, the alternative age model for

the Pleistocene Vrica section is untenable. The Vrica section contains a continuous Pleistocene succession from 1.81 (i.e., the Pliocene/Pleistocene boundary) to 1.21 Ma.

More than 10 yr after its formal designation as a Pliocene/Pleistocene boundary stratotype, the Vrica section can now be considered as a (land based) standard reference section for the early Pleistocene, because it is shown to contain a continuous succession. In addition, the continuity makes Vrica an appropriate section for defining the Santernian/Emilian (S/E) boundary, even though the criterion proposed by Pasini and Colalongo (1994; i.e., the FO of *H. balthica*), is less suitable because of difficulties encountered in independently confirming its position in the Vrica section (see Lourens et al., 1996a) and the diachronous nature of this event even within the Mediterranean (Fig. 4B). In contrast, the blG is (near-)synchronous in at least the eastern Mediterranean and equatorial Atlantic, and, even on a global scale, it still gives a fair approximation of the position of the S/E boundary. Nevertheless, the observed blG diachroneity of ±135 k.y. between the eastern Mediterranean and the North Atlantic DSDP Site 607 is almost half of the total duration (about 315 k.y.) of the Santernian as informally defined in the Vrica section. In the absence of an appropriate biostratigraphic datum plane or magnetic polarity reversal, cyclostratigraphy may guide the selection of the "golden spike" and therefore, a precession-related sapropel may represent a suitable position to define the S/E boundary. It would thereby follow the Pliocene/Pleistocene (Aguirre and Pasini, 1985), Piacenzian/Gela-

sian (Rio et al., 1994) and Zanclean/Piacenzian (Cita et al., 1996) boundary definitions.

ACKNOWLEDGMENTS

REFERENCES

Aguirre, E., and Pasini, G., 1985. The Pliocene-Pleistocene boundary. *Episodes,* 8:11–120.

Bickert, T., Curry, W.B., and Wefer, G., 1997. Late Pliocene to Holocene (2.6–0 Ma) western equatorial Atlantic deep-water circulation: inferences from benthic stable isotopes. *Proc. ODP, Sci. Results,* 154: College Station, TX (Ocean Drilling Program), 239–253.

Cita, M.B., Rio, D., Hilgen, F., Castradori, D., Lourens, L., and Vergerio, P.P., 1996. Proposal of the Global Boundary Stratotype Section and Point (GSSP) of the Piacenzian Stage (middle Pliocene). *Int. Comm. on Stratigr. Subcomm. on Neogene Stratigr.*

Emeis, K.-C., Robertson, A.H.F., Richter, C., et al., 1996. *Proc. ODP, Init. Repts.,* 160: College Station, TX (Ocean Drilling Program).

Hilgen, F.J., 1991. Astronomical calibration of Gauss to Matuyama sapropels in the Mediterranean and implication for the geomagnetic polarity time scale. *Earth Planet. Sci. Lett.,* 104:226–244.

Laskar, J., Joutel, F., and Boudin, F., 1993. Orbital, precessional, and insolation quantities for the Earth from −20 Myr to +10 Myr. *Astron. Astrophys.,* 270:522–533.

Lourens, L.J., Hilgen, F.J., Raffi, I., and Vergnaud-Grazzini, C., 1996a. Early Pleistocene chronology of the Vrica section (Calabria, Italy). *Paleoceanography,* 11:797–812.

Lourens, L.J., Hilgen, F.J., Zachariasse, W.J., van Hoof, A.A.M., Antonarakou, A., and Vergnaud-Grazzini, C., 1996b. Evaluation of the Plio-Pleistocene astronomical time scale. *Paleoceanography,* 11:391–413.

Pasini, G., and Colalongo, M.L., 1994. Proposal for the erection of the Santernian/Emilian boundary-stratotype (lower Pleistocene) and new data on the Pliocene-Pleistocene boundary-stratotype. *Boll. Soc. Paleont. Ital.,* 33:101–120.

Raffi, I., Backman, J., Rio, D., and Shackleton, N.J., 1993. Plio-Pleistocene nannofossil biostratigraphy and calibration to oxygen isotopes stratigraphies from Deep Sea Drilling Project Site 607 and Ocean Drilling Program Site 677. *Paleoceanography,* 8:387–408.

Rio, D., Sprovieri, R., and Di Stefano, E., 1994. The Gelasian stage: a proposal for a new chronostratigraphic unit of the Pliocene series. *Riv. Ital. Paleontol. Stratigr.,* 100:103–124.

Verhallen, P.J.J.M., 1991. Late Pliocene to early Pleistocene Mediterranean mud-dwelling foraminifera; influence of a changing environment on community structure and evolution. *Utrecht Micropaleontol. Bull.,* 40:1–220.
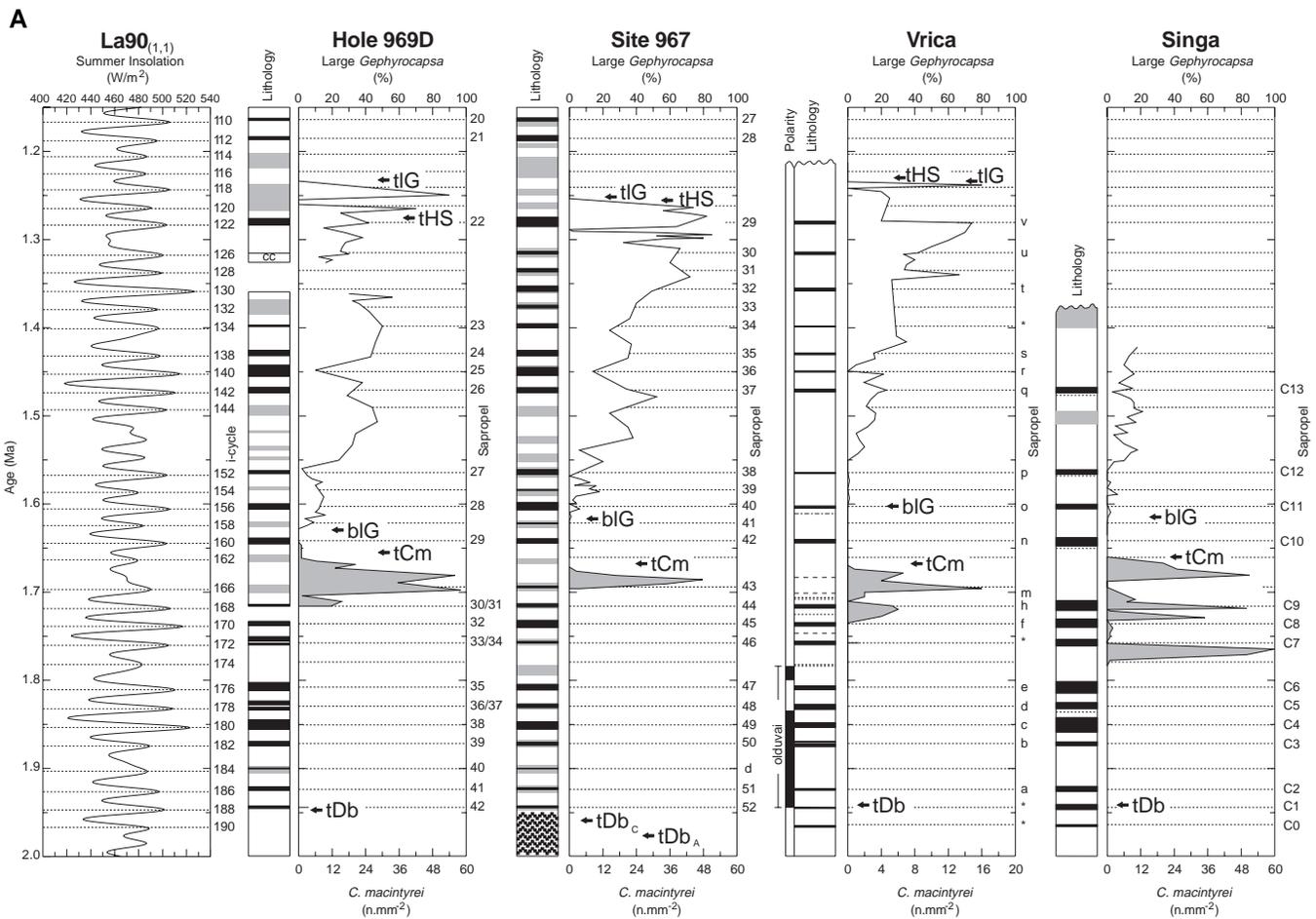
Figure 4. Comparison of the sapropel patterns and biostratigraphic datums between ODP Site 967 and Hole 969D, and the Vrica and Singa sections based on the continuous age model of Lourens et al. (1996a). See Figure 2 for definitions. **A.** Calcareous nannofossil events. **B.** Planktonic foraminifers and *Hyalinea balthica*. Numbers within the third column from right refer to oxygen isotopic stages.

Figure 4 (continued).